A BRINKMAN PENALIZATION LATTICE BOLTZMANN METHOD SIMULATION OF THE FLOW OVER A POROUS BACKWARD-FACING STEP

Léo Roussel[1*], **Chloé Mimeau**[2], **Simon Marié**[1]
[1]Laboratoire DynFluid
Conservatoire National des Arts et Métiers, 2 rue Conté, Paris 75003, France.
[2]Laboratoire M2N
Conservatoire National des Arts et Métiers, 2 rue Conté, Paris 75003, France.
*Corresponding author: leo.roussel@lecnam.net

INTRODUCTION

Turbulent flows over porous media are commonly found in nature and thus make up for numerous applications in areas such as geophysics, chemical engineering and meteorology. However, this kind of flows is particularly difficult to study because of the large range of scales involved. In numerical simulations, resolving all scales down to the pore size is prohibitively expensive in an industrial context. Instead, upscaling methods can be used that only consider the flow on a macroscopic, pore-averaged scale. These techniques rely on effective coefficients that characterize the effect of the porous medium on the flow. One such approach, called the Brinkman penalization method, introduces a forcing term in the Navier-Stokes equations that leaves the flow unaltered in the free-fluid region Ω_f, and that penalizes the flow in the porous region Ω_p, depending on the medium's porosity ϕ and dimensionless permeability, also known as the Darcy number Da. This formulation allows the description of the flow with a single equation valid in the whole domain. In this work, the Brinkman penalization method is implemented within an in-house Lattice Boltzmann Method (LBM) solver and is used to simulate the flow past a porous backward-facing step (BFS). The influence of the permeability of the step is evaluated by comparison with the flow past a solid step. The results are validated against the experimental data of Klotz et al. [1] on the flow behind a BFS with a 10 PPI (Pores Per Inch) porous insert, in the transitional regime, at a Reynolds number $\mathrm{Re} \equiv U_0 h/\nu = 510$, where U_0 is the centerline velocity and h is the step height. Then, additional simulations are carried out at $\mathrm{Re} = 1150$ to study the influence of the porous step on the turbulent flow.

NUMERICAL SETUP

In this work, a LBM scheme is used to implement the Brinkman penalization method. The Multiple Relaxation Times (MRT) collision model and the nineteen velocities lattice (D3Q19) are chosen in order to recover the athermal Navier-Stokes equations for small Mach numbers [2] (set to $\mathrm{Ma} = 0.17$ in the present work). In the framework of the Brinkman penalization method, the governing equations are supplemented with the following forcing term:

$$\boldsymbol{\Gamma} = \begin{cases} \dfrac{\phi}{\mathrm{ReDa}}\boldsymbol{u} + \dfrac{\phi c_F}{\sqrt{\mathrm{Da}}}|\boldsymbol{u}|\boldsymbol{u}, & \boldsymbol{x} \in \Omega_p, \\ 0, & \boldsymbol{x} \in \Omega_f. \end{cases} \tag{1}$$

The effective coefficients are matched with those of the 10 PPI insert in the experiment of Klotz et al. [1]: the porosity is set to $\phi = 0.98$, the Darcy number based on step height is set to $\mathrm{Da} = 3.3 \times 10^{-3}$, and the Forchheimer coefficient is set to $c_F = 0.05$. The computational domain is sketched in Figure 1. A Blasius boundary layer profile is prescribed at the inlet with the boundary-layer thickness estimated from Klotz et al. [1] to be roughly equal to $\delta_{99} \simeq 9\,\mathrm{mm}$. A convective outflow condition is used at the outlet, with a propagation velocity U_{out} set to the Blasius boundary layer profile with the same boundary-layer thickness as the inflow. The length of the domain is $120h$ in the solid case and $130h$ in the porous case and the height of the domain is $12h$, yielding an expansion ratio of $\mathrm{ER} \equiv L_y/(L_y - h) \simeq 1.1$. No-slip conditions are applied on the top and bottom walls and periodicity is imposed in the span. The choice of geometry and boundary conditions was found to be essential for an accurate restitution of the spectral characteristics. In particular, simulations run in a smaller domain or with a free-slip condition on the top boundary were unable to predict the appearance of the low frequency St_1 (described in the following section) in the solid BFS case.

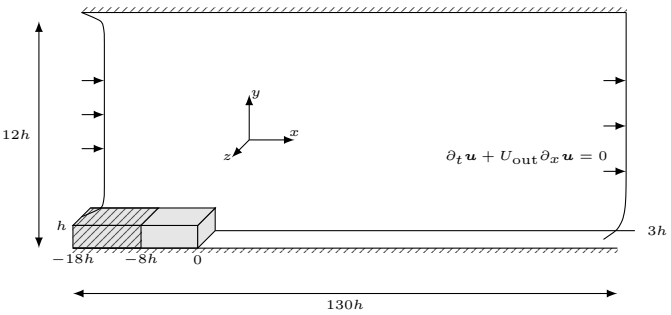

Figure 1: Sketch of the computational domain and the boundary conditions. The porous insert is represented by the light-grey block and solid boundary conditions are materialized by hatched lines.

COMPARISON WITH EXPERIMENT

In order to evaluate the ability of the model to correctly reproduce the effect of the porous step, a reference case with a solid impermeable step is also considered. The numerical results in the porous case and control case (solid) are both compared against the experimental ones reported in [1]. The spectral amplitudes in the experimental and in the two numerical cases are shown in Figure 2 as a function of streamwise location x/h and Strouhal num-

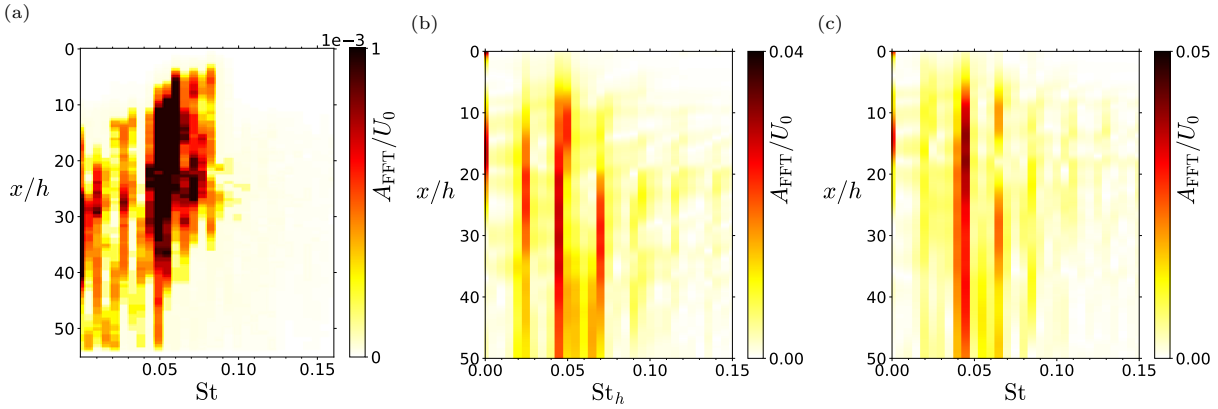

Figure 2: Discrete Fourier transform amplitude of the wall-normal instantaneous velocity at cross-flow location $(y, z) = (0.7h, 1.5h)$. (a) Experimental data for the 10 PPI porous insert at $\mathrm{Re} = 510$ from [1]. Present simulation results with (b) the solid step and (c) the porous step.

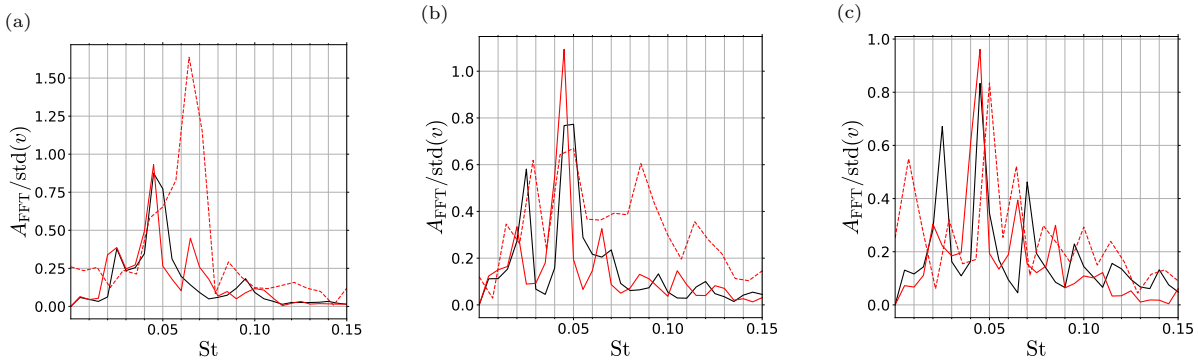

Figure 3: Discrete Fourier transform amplitude of the wall-normal instantaneous velocity at locations (a) $x/h = 5.5$, $y/h = 1.2$. (b) $x/h = 14.9$, $y/h = 0.9$. (c) $x/h = 22.6$, $y/h = 1.1$. Red dashed line denotes the experimental result of Klotz et al. [1] for the 10 PPI porous insert. Black continuous line denotes the simulation result in the solid case, red continuous line denotes the simulation result in the porous case.

ber $\mathrm{St} \equiv fh/U_0$. In the experimental data related to the porous BFS, two peak frequencies are measured at respective Strouhal numbers $\mathrm{St}_1 \simeq 0.03$ and $\mathrm{St}_2 \simeq 0.05$. It is argued in Klotz et al. [1], that the low frequency St_1 may be tied to a Tollmien-Schlichting instability of the reattaching boundary layer. Past the reattachment point, the local velocity profiles can be matched with Falkner-Skan boundary layers, and the measured frequencies in this neighborhood agree with the most amplified frequency found by linear stability of the Falkner-Skan basic flows. On the other hand, the high frequency St_2, when scaled by the momentum thickness at separation, is found equal to the most amplified frequency of the mixing layer [6] at some critical Reynolds number before eventually decreasing. This suggests that the separated shear layer undergoes a Kelvin-Helmholtz instability upon its initial roll-up. The authors explain that these two peaks were found to be roughly equivalent in the solid case. However, as the permeability of the insert increases, the higher frequency peak tended to become more energetic with respect to the lower frequency one, thus enhancing the Kelvin-Helmholtz instability. This trend is most pronounced in the case of the 10 PPI insert, as can be seen in the spectrum displayed in Figure 2a, where the second peak is clearly prevailing over the first one throughout the full streamwise range. This influence of the porous insert with respect to the solid one was correctly recovered in the present numerical simulations. Indeed, although the Strouhal numbers were found to be slightly lower than in the experimental data, the presence of two peaks at respective frequencies $\mathrm{St}_1^{\mathrm{num}} = 0.02$ and $\mathrm{St}_2^{\mathrm{num}} = 0.045$ is in fact observed in both Figures 2b (solid) and 2c (porous), and the relative magnitude of the energy associated to each peak is similar to the experimental observations. Indeed, in the solid case in Figure 2b, the two frequencies share roughly equivalent amplitudes, whereas in the porous case in Figure 2c, the higher frequency $\mathrm{St}_2^{\mathrm{num}}$ does have a much larger amplitude than the lower frequency at $\mathrm{St}_1^{\mathrm{num}}$. A closer inspection is carried out in the porous case in Figure 3, where a side-by-side comparison is shown of the experimental and numerical Fourier transform amplitudes, normalized by their respective standard deviation. Though the numerical method seems unable to retrieve the spectrum at a spatial location close to the porous insert as shown in Figure 3a (that may be attributed to an effect of the particular pore geometry of the insert close to the interface, which is not

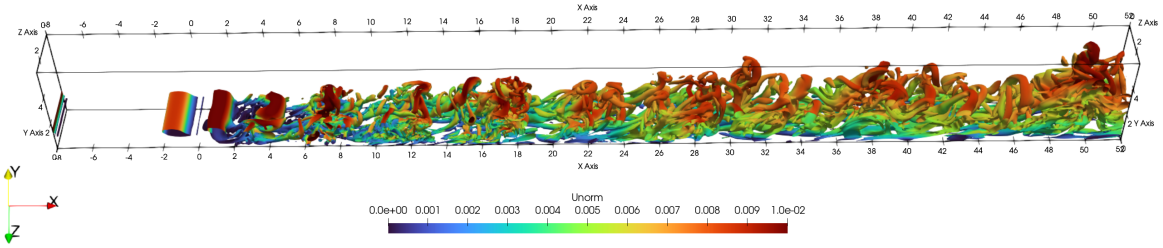

Figure 4: Iso-surfaces of λ_2-criterion colored by the norm of the velocity field at $\mathrm{Re} = 1150$. The porous insert is located at $-8 \leq x/h \leq 0$.

taken into account with the present Brinkman penalization method), this does not alter the ability of the model to correctly predict the dynamics farther downstream, as evidenced in Figures 3b and 3c.

EFFECT OF PERMEABILITY ON TURBULENCE

The reliability of the Brinkman model was confirmed in the prediction of the influence of the porous wall on the downstream flow thanks to the previous validation effort. The next step is to study the effect of the porous insert on the flow in the turbulent case. Here, some preliminary results are discussed at $\mathrm{Re} = 1150$, while leaving the material properties of the medium unchanged to witness the evolution for increasing Reynolds number. A snapshot of the flow field is shown in Figure 4, which shows the vortex roll-up initiated upstream of the the porous step's edge at $x/h = 0$, in contrast to the previous case where it occurs some distance past the step edge as seen in the spectra. This peculiarity is corroborated in the spectrum in Figure 5, where a marked peak at $\mathrm{St} = 0.14$, extending ahead of the step edge, is amplified over a significant range in the streamwise direction. Upon scaling with the momentum thickness θ at the step edge, this frequency is found to be equal to $\mathrm{St}_\theta \equiv f\theta/U_0 \simeq 0.014$, which lies close to the natural frequency of the mixing layer [6]. This may hint at a possibly destabilizing effect of the porous step, as the transition to turbulence would then be triggered by the Kelvin-Helmholtz flow instability. The comparison with the solid case and a finer analysis of the mechanisms at play are currently underway to confirm this hypothesis.

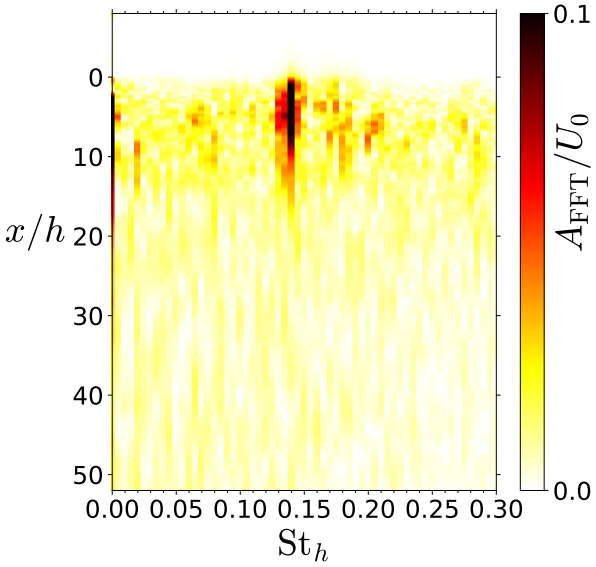

Figure 5: Discrete Fourier transform amplitude of the wall-normal instantaneous velocity at $\mathrm{Re} = 1150$, at cross-flow location $(y, z) = (0.7h, 1.5h)$.

REFERENCES

[1] Klotz, L., Bukowski, K., and Gumowski, K. : Influence of porous material on the flow behind a backward-facing step: experimental study. *Journal of Fluid Mechanics*, **998**, A31 (2024).

[2] Shan, X., Yuan, X.-F., and Chen, H. : Kinetic theory representation of hydrodynamics: a way beyond the Navier–Stokes equation. *Journal of Fluid Mechanics*, **550**, 413–441 (2006).

[3] Breugem, W. P., Boersma, B. J., and Uittenbogaard, R. E. : The influence of wall permeability on turbulent channel flow. *Journal of Fluid Mechanics*, **562**, 35-72 (2006).

[4] Luminari, N., Zampogna, G. A., Airiau, C., and Bottaro, A. : A penalization method to treat the interface between a free-fluid region and a fibrous porous medium. *Journal of Porous Media*, **22** (9), 1095-1107 (2019).

[5] Bendali, Y., Chabanon, M., Holka, Q., and Goyeau, B. : Macroscopic Orientation of Inertial Flows in Porous Media. *Transport in Porous Media*, **152** (8), 51 (2025).

[6] Ho, C. M., and Huerre, P. : Perturbed free shear layers. *Annual review of fluid mechanics*, ***16***, *365-424 (1984).*